Computer simulation studies of the speckle correlations of light scattered from a random array of scatterers: Scalar wave approximation

A. R. McGurn[1] and A. A. Maradudin[2]
[1]*Department of Physics, Western Michigan University, Kalamazoo, Michigan 49008*
[2]*Department of Physics and Astronomy, University of California, Irvine, California 92697*
(Received 7 July 2000; revised manuscript received 2 May 2001; published 5 October 2001)

Two computer simulation studies of the speckle correlations in the light scattered from a volume disordered dielectric medium consisting of a random array of dielectric spheres are made. In both studies light is treated in the scalar wave approximation, and the wavelength of the light is taken to be much greater than the radius of the dielectric spheres. In one study, the scattering medium is formed by placing dielectric spheres of radius R and dielectric constant ϵ randomly in space. The spheres occupy space uniformly, under the provision that no two spheres overlap. In a second study, the scattering medium is formed by placing dielectric spheres of radius R and dielectric constant ϵ randomly on the vertices of a simple cubic lattice so that a fixed fraction of the vertices is occupied by the spheres. The lattice constant of the simple cubic lattice is taken to be of the order of magnitude of the wavelength of light in vacuum. In both studies the the volume filling fraction is the same, and the region outside the spheres is vacuum. The field equations are integrated numerically to determine the scattered fields, and these fields are used to calculate the speckle correlation function defined by $C(\vec{q},\vec{k}|\vec{q}',\vec{k}')=\langle[I(\vec{q}|\vec{k})-\langle I(\vec{q}|\vec{k})\rangle][I(\vec{q}'|\vec{k}')-\langle I(\vec{q}'|\vec{k}')]\rangle$. Here $I(\vec{q}|\vec{k})$ is proportional to the differential scattering coefficient for the elastic scattering of light of wave vector $\vec{k}$ into light of wave vector $\vec{q}$, and $\langle\ \rangle$ indicates an average over an ensemble of random systems. Results are presented for $C(\vec{q},\vec{k}|\vec{q}',\vec{k}')$ with particular attention paid to regions of $\vec{k}$ space in which either the $C^{(1)}$ or $C^{(10)}$ contributions dominate the correlator.

DOI: 10.1103/PhysRevB.64.165204 PACS number(s): 71.55.Jv, 78.90.+t, 78.20.Bh

I. INTRODUCTION

In this paper we present computer simulation studies of features in the speckle pattern of light scattered by volume disordered media. Of specific interest are the correlations that exist between the differential scattering cross sections for two different sets of angles of incidence and scattering. These correlations are measured by the speckle correlator[1–10] $C(\vec{q},\vec{k}|\vec{q}',\vec{k}')=\langle[I(\vec{q}|\vec{k})-\langle I(\vec{q}|\vec{k})\rangle][I(\vec{q}'|\vec{k}')-\langle I(\vec{q}'|\vec{k}')\rangle]\rangle$, where $I(\vec{q}|\vec{k})$ is proportional to the differential scattering coefficient for the elastic scattering of light of wave vector $\vec{k}$ into light of wave vector $\vec{q}$, and $\langle\ \rangle$ denotes an average over a statistical ensemble of random configurations. Two studies are presented, one for the light scattered by a homogeneous randomly disordered medium and one for the light scattered by a random medium that is periodic on average. The media we study are formed by placing dielectric spheres of radius R and dielectric constant ϵ in space at a fixed volume filling fraction. The spheres, which are not allowed to overlap, have a radius much smaller than the wavelength of the light in vacuum, and the region outside the spheres is taken to be vacuum.

The features in the speckle correlator, $C(\vec{q},\vec{k}|\vec{q}',\vec{k}')$, of the scattered light that are of interest are the short-range contributions $C^{(1)}(\vec{q},\vec{k}|\vec{q}',\vec{k}')$ (Refs. 1–9) and $C^{(10)}(\vec{q},\vec{k}|\vec{q}',\vec{k}')$.[10–12] These features dominate $C(\vec{q},\vec{k}|\vec{q}',\vec{k}')$, so that to an excellent approximation we study $C(\vec{q},\vec{k}|\vec{q}',\vec{k}')\approx C^{(1)}(\vec{q},\vec{k}|\vec{q}',\vec{k}')+C^{(10)}(\vec{q},\vec{k}|\vec{q}',\vec{k}')$. The contribution $C^{(10)}$ is a feature in the speckle correlator for volume scattering that has recently been predicted on the basis of a diagrammatic perturbation theory for a homogeneous random disordered medium.[10–12] The general features of $C^{(1)}$ have been studied both theoretically and experimentally in other types of volume and surface disordered optical systems.[1–9]

The present computer simulation studies are intended to complement and support the Green's-function study of $C^{(10)}$ and to provide a comparison of this term to the $C^{(1)}$ term occurring in scattering from the same statistical system. In addition, different features of these correlators, associated with the periodic on average system, are presented. The computer simulation yields an essentially exact solution for the speckle correlator, and is not subject to the approximations of a diagrammatic perturbation-theory treatment. Since the general properties of the correlator are faithfully represented by simulation results, a meaningful comparison of $C^{(10)}$ with $C^{(1)}$ in the same bulk randomly disordered optical system can be made. An interesting aspect of the present set of simulation studies is the comparison of the results for the homogeneous random disordered and the periodic on average random system. The $C^{(1)}$ and $C^{(10)}$ terms of the periodic on average system are found to exhibit interesting features not observed in these terms for the uniformly random system.

Theoretical work on speckle correlations is concerned with computing the features in the speckle correlator arising from a variety of different types of scattering processes and classifying the contributions of these processes to the general speckle correlator $C(\vec{q},\vec{k}|\vec{q}',\vec{k}')$. Short-, long-, and infinite-range terms denoted by $C^{(1)},C^{(2)},C^{(3)}$, respectively, were first shown to contribute to the total speckle correlator of the

scattered light and to arise from distinctly different types of scattering processes.[1–12] The magnitude of the contribution of each of these terms, $C^{(i)}$ for $i=1,2,3$, was found to decrease rapidly with increasing i. More recently, additional features arising from different types of scattering processes have been predicted in the speckle correlator.[10–12] These are the $C^{(10)}$ short-range and the $C^{(1.5)}$ long-range terms. The $C^{(10)}$ contribution is found to be of the same order of magnitude as the $C^{(1)}$ contribution, but the magnitude of the $C^{(1.5)}$ term is found to be intermediate between those of the $C^{(1)}$ and $C^{(10)}$ terms and the much smaller $C^{(2)}$ term. For the systems we treat in this paper the $C^{(1.5)}$, $C^{(2)}$, $C^{(3)}$ contribution are masked by the statistical noise in our simulations.

$C^{(1)}$ first occurs in the lowest order in the perturbative expansion of the speckle correlator in powers of the volume disorder. $C^{(1)}$ contains phase coherent peaks in wave-vector space known as the memory and time-reversed memory effects in the angular speckle correlator.[1–9] $C^{(10)}$ first occurs in the same order in the expansion of the speckle correlator in powers of the volume disorder[10–12] as does $C^{(1)}$. Because of the scattering geometries involved, the $C^{(10)}$ term, however, does not display phase-coherent effects. $C^{(10)}$ has been studied by us in the scattering of light from randomly rough surfaces, and in the context of a Green's-function perturbation theory in the scattering from volume disordered media.[10]

The remaining $C^{(1.5)}$, $C^{(2)}$, and $C^{(3)}$ terms occur as increasingly higher-order terms in the perturbation-theory expansion of C in the random disorder. $C^{(1.5)}$ and $C^{(2)}$ contain a number of features that can be related to multiple-scattering processes.[10–12] $C^{(3)}$, which is the weakest contribution to the speckle correlator, is a smoothly varying function in wave-vector space.

The general speckle correlator is the sum of the five contributions mentioned above. This paper will concentrate on the $C^{(1)}$ and $C^{(10)}$ contributions. These dominate the speckle correlator, and are the only contributions to the speckle correlator observed in our simulation studies. A comparison of $C^{(1)}$ and $C^{(10)}$ is made for several values of the dielectric constant in the limit that the wavelength of the incident light is much larger than the radius of the dielectric spheres. A comparison is also made between $C^{(1)}$ and $C^{(10)}$ for a homogeneous random system and a random system that is periodic on average.

The outline of this paper is as follows. In Sec. II the model for bulk elastic scattering is presented, and the calculation of the scattering cross section in this model is discussed. In Sec. III the definition of the speckle correlator $C(\vec{q},\vec{k}|\vec{q}',\vec{k}')$ is presented, and the $C^{(1)}$, $C^{(10)}$ contributions to it are discussed. Numerical results for the scattering cross section and the angular speckle correlator in the light elastically scattered are then presented and discussed. A discussion and comparison is given of the simulation results for the $C^{(1)}$ and $C^{(10)}$ contributions to the speckle correlator. In Sec. IV our conclusions are presented.

II. MODEL AND DIFFUSE SCATTERING

We consider a bulk random dielectric medium composed of an array of spheres of dielectric constant ϵ and radius R that are randomly distributed in space. The region outside the spheres is vacuum, and a volume filling fraction ρ of space is occupied by the spheres. Two different systems are studied. In the first system (homogeneous random system) the spheres randomly occupy space uniformly with the condition that they do not overlap. In the second system (periodic on average random system) the spheres randomly occupy the sites of a simple cubic lattice of lattice constant $a \gg R$. In both cases the wavelength of the light in vacuum is taken to be much larger than the radius of the spheres, i.e., $\lambda \gg R$. This is the fundamental restriction in our simulation and it is made to simplify the mathematical treatment of the scattering cross section of the electromagnetic waves from the individual spheres in the array of scatterers [see Eqs. (9)–(16) below].

Both of these systems are described by a position-dependent dielectric constant of the form

$$\epsilon(\vec{r}) = 1 + \delta\epsilon(\vec{r}), \tag{1}$$

where

$$\delta\epsilon(\vec{r}) = (\epsilon - 1)\sum_{l} S[\vec{r} - \vec{r}(l)], \tag{2}$$

$$S(\vec{r}) = \begin{cases} 1, & |\vec{r}| \leqslant R \\ 0, & \text{otherwise,} \end{cases} \tag{3}$$

and $\{\vec{r}(l)\}$ are the position vectors of the three-dimensional array of spheres. In the computer simulation studies presented below, a finite volume of the system described by Eq. (2) is considered. The far-field scattering from the finite volume of randomly arrayed spheres is computed and used to compute the speckle correlator. An average is made of the differential scattering coefficient and the speckle correlator over a large number of realizations of the random system. The resulting averages are taken as approximations of these quantities for the infinite system.

To simplify the mathematics, the propagation of light will be treated in the scalar wave approximation.[13] In this approximation the scalar wave field, $\psi(\vec{r},t) = \psi(\vec{r})\exp(-i\omega t)$, is determined by

$$\left[\Delta - \frac{\epsilon(\vec{r})}{c^2}\frac{\partial^2}{\partial t^2}\right]\psi(\vec{r},t) = 0, \tag{4}$$

the field energy density is given by

$$\rho(\vec{r}) = \frac{1}{8\pi}\left(\frac{\epsilon(\vec{r})}{c^2}\left|\frac{\partial\psi(\vec{r},t)}{\partial t}\right|^2 + |\nabla\psi(\vec{r},t)|^2\right), \tag{5}$$

and the energy current is given by

$$\vec{J}(\vec{r}) = -\frac{1}{8\pi}\left(\frac{\partial\psi^*(\vec{r},t)}{\partial t}\nabla\psi(\vec{r},t) + \frac{\partial\psi(\vec{r},t)}{\partial t}\nabla\psi^*(\vec{r},t)\right). \tag{6}$$

The solution to the scattering problem defined by Eqs. (1)–(6) can be formally written in terms of the Green's func-

tion of the Helmholtz equation for the propagation of the scalar wave field in vacuum. This Green's function is defined as the solution of

$$\left[\Delta+\left(\frac{\omega}{c}\right)^2\right]G(\vec{r},\vec{r'})=-4\pi\delta(\vec{r}-\vec{r'}), \tag{7}$$

subject to an outgoing wave boundary condition at infinity. The well-known solution is

$$G(\vec{r}|\vec{r'})=\frac{e^{i(\omega/c)|\vec{r}-\vec{r'}|}}{|\vec{r}-\vec{r'}|}. \tag{8}$$

In terms of $G(\vec{r}|\vec{r'})$ the scattering solution of Eq. (4) is

$$\psi(\vec{r})=\psi_{inc}(\vec{r})+\frac{1}{4\pi}\left(\frac{\omega}{c}\right)^2\int d^3r'\,G(\vec{r}|\vec{r'})\,\delta\epsilon(\vec{r'})\,\psi(\vec{r'}), \tag{9}$$

where $\psi_{inc}(\vec{r})$ is the incident field, which we shall take to be a plane wave. Substituting Eqs. (2) and (3) into Eq. (9), we find

$$\psi(\vec{r})=\psi_{inc}(\vec{r})+\frac{1}{4\pi}\left(\frac{\omega}{c}\right)^2(\epsilon-1)\sum_l\int d^3r'\,G(\vec{r}|\vec{r'})\times S[\vec{r'}-\vec{r}(l)]\psi(\vec{r'}). \tag{10}$$

If the radius R of the spheres is small compared to the wavelength of the light in vacuum, $\psi(\vec{r'})$ varies slowly over the volume of the individual dielectric spheres, and we can rewrite Eq. (10) as

$$\psi(\vec{r})=\psi_{inc}(\vec{r})+\frac{\epsilon-1}{4\pi}\left(\frac{\omega}{c}\right)^2\sum_l\psi[\vec{r}(l)]\times\int_V d^3u\,G[\vec{r}|\vec{r}(l)+\vec{u}], \tag{11}$$

where V is the volume of a sphere of radius R centered at the origin of coordinates.

The differential scattering cross section for the scattering of scalar waves from the random volume disorder is obtained from the ratio of the scattered scalar wave current and the incident current. The scattering solution of Eq. (4) as represented in Eq. (9) is of the form

$$\psi(\vec{r})=\psi_{inc}(\vec{r})+\psi_{sc}(\vec{r}), \tag{12}$$

where $\psi_{sc}(\vec{r})$ is the scattered wave. For an incident plane wave of the form

$$\psi_{inc}(\vec{r})=\exp(i\vec{k}\cdot\vec{r}), \tag{13}$$

the scattered wave is given in the far field by

$$\psi_{sc}(\vec{r})=f(\hat{q},\hat{k})\frac{\exp(ik_0r)}{r}. \tag{14}$$

Here $k_0=\omega/c$, and $\vec{k}$ and $\vec{q}$ are the wave vectors of the incident and scattered fields. The scattering cross section is then

$$\frac{d\sigma}{d\Omega}(\vec{q}|\vec{k})=|f(\hat{q},\hat{k})|^2. \tag{15}$$

From Eq. (11) the field scattered from the array of spheres is given in the far field by

$$\psi_{sc}(\vec{r})\approx\frac{\epsilon-1}{4\pi}\left(\frac{\omega}{c}\right)^2 3V\frac{j_1(k_0R)}{k_0R}\frac{e^{ik_0r}}{r}\sum_{k,l}e^{-ik_0\hat{r}\cdot\vec{r}(k)}\times\left[\overleftrightarrow{I}-\frac{\epsilon-1}{4\pi}\left(\frac{\omega}{c}\right)^2\overleftrightarrow{M}\right]^{-1}_{\vec{r}(k),\vec{r}(l)}\psi_{inc}[\vec{r}(l)], \tag{16}$$

where the matrix elements of $\overleftrightarrow{M}$ at $\vec{r}(k),\vec{r}(l)$ are

$$M_{\vec{r}(k),\vec{r}(l)}=\int_V d^3u\,G[\vec{r}(k)|\vec{r}(l)+\vec{u}]. \tag{17}$$

In Eqs. (16) and (17) $\hat{r}=(\sin\theta_s\cos\phi_s,\sin\theta_s\sin\phi_s,\cos\theta_s)$, for polar and azimuthal scattering angles θ_s, ϕ_s, and $j_1(x)$ is the spherical Bessel function of order 1.

III. SPECKLE CORRELATIONS

The angular correlator for the scattering of light measures the correlations in the speckle patterns arising from two different scatterings of light from the same randomly disordered medium. The angular intensity correlator is defined in terms of the fluctuations in the differential scattering cross section given by Eq. (15) from its value averaged over many realizations of the random system. These fluctuations are

$$\delta I(\vec{q}|\vec{k})=\left[\frac{\partial\sigma}{\partial\Omega}(\vec{q}|\vec{k})-\left\langle\frac{\partial\sigma}{\partial\Omega}(\vec{q}|\vec{k})\right\rangle\right], \tag{18}$$

where $\langle\,\rangle$ represents an average over the ensemble of realizations of the random system and $I(\vec{q}|\vec{k})=(\partial\sigma/\partial\Omega)(\vec{q}|\vec{k})$. In terms of $\delta I(\vec{q}|\vec{k})$, the angular speckle correlator is

$$C(\vec{q},\vec{k}|\vec{q}',\vec{k}')=\langle\delta I(\vec{q}|\vec{k})\,\delta I(\vec{q}'|\vec{k}')\rangle=\left[\left\langle\frac{\partial\sigma}{\partial\Omega}(\vec{q}|\vec{k})\frac{\partial\sigma}{\partial\Omega}(\vec{q}'|\vec{k}')\right\rangle-\left\langle\frac{\partial\sigma}{\partial\Omega}(\vec{q}|\vec{k})\right\rangle\times\left\langle\frac{\partial\sigma}{\partial\Omega}(\vec{q}'|\vec{k}')\right\rangle\right]. \tag{19}$$

The scattering geometries involved in defining the correlator in Eq. (19) are shown in Fig. 1.

In the studies below results for the homogeneous random systems are obtained from runs involving 125 spheres, and results for the periodic on average studies are obtained from runs on systems of 225 dielectric spheres. The volume filling fraction in both of these studies is fixed at $\rho=0.000\,247$. The spheres occupy a cubic volume that is centered at the origin of spatial coordinates, with faces parallel to the $x-y$, $y-z$,

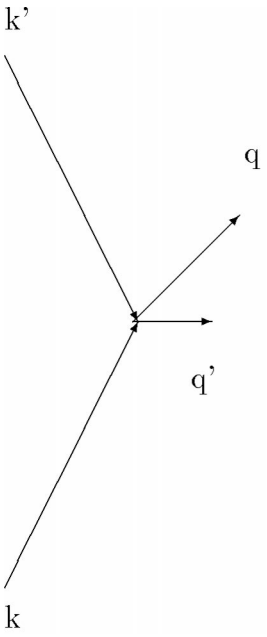

FIG. 1. Schematic representation of the wave-vector geometry for the correlation between two elastic scattering processes in three-dimensional space. One process involves the scattering of an incident wave with wave vector $\vec{k}$ into an outgoing wave with wave vector $\vec{q}$, and the other process involves the scattering of an incident wave with wave vector $\vec{k}'$ into an outgoing wave with wave vector $\vec{q}'$. The scattering system is at the vertex.

and $x-z$ planes. The radius of the spheres is taken to be $R/\lambda=0.064$, where λ is the wavelength of light in vacuum. For the majority of runs $\epsilon=-9$, but additional runs for $\epsilon=-2$, 2, 9 were also made. We have considered the cases of negative dielectric constants because metal particles can have negative dielectric constants. While the physical effects discussed below are observed for particles with both negative and positive dielectric constants, the effects show up best in systems of particles with negative dielectric constants. This should be a point of interest to those who would be interested in observing the effects predicted in the computer simulations studies presented below. For the periodic on average system the spheres are taken to occupy randomly the sites of a simple cubic lattice with lattice constant $a/\lambda \approx 1$. The speckle correlators are obtained by averaging over results from 500 or 1000 realizations of the disordered system.

For *s*-wave scattering from the spheres in our model, the solutions of the Helmholtz equation inside the spheres are proportional to the spherical Bessel function $j_0[(\epsilon)^{1/2}(\omega/c)r]$ for positive ϵ and the modified spherical Bessel function $i_0[(-\epsilon)^{1/2}(\omega/c)r]$ for negative ϵ. For positive dielectric spheres $j_0[(\epsilon)^{1/2}(\omega/c)R]/j_0(0)=\sin[(\epsilon)^{1/2}(\omega/c)R]/[(\epsilon)^{1/2}(\omega/c)R]$ is a measure of the validity of the approximation in going from Eq. (10) to Eq. (11). For $\epsilon=9$ this ratio is 0.77 and for $\epsilon=2$ this ratio is 0.95. For negative dielectric spheres $i_0[(-\epsilon)^{1/2}(\omega/c)R]/i_0(0)=\sinh[(-\epsilon)^{1/2}(\omega/c)R]/[(-\epsilon)^{1/2}(\omega/c)R]$ is a measure of the validity of the approximation made in going from Eq. (10) to Eq. (11). For $\epsilon=-9$ this ratio is 1.26 and for $\epsilon=-2$ this ratio is 1.05. The $\epsilon=\pm 9$ results are near the limits of the validity of the approximation but should give reliable representations of the speckle patterns from experimental realizations of these systems.

A. Scattering cross sections

We first present the differential scattering cross sections for the two different models. In Fig. 2(a) the differential scattering cross section is presented for the homogeneous random system. The wave vectors of the incident and scattered waves are, respectively, $\vec{k}=k_0(1,0,0)$ and $\vec{q}=k_0(\cos\phi_s,\sin\phi_s,0)$, and results are shown for several values of ϵ. In general the diffuse scattering cross sections are seen to be fairly isotropic in space. This is due to the small ratio of the dielectric sphere radius to the wavelength of light. This favors *s*-wave scattering from the individual spheres which, along with the uniform random distribution of spheres in space, gives rise to an isotropic cross section.

For comparison, in Fig. 2(b) the differential scattering cross section for several values of the dielectric constant is shown for a random system that is periodic on average. In these calculations we have taken $a/\lambda=1$. Consequently, the *s*-wave scattering from an individual dielectric sphere can be affected by the average periodicity of the system to give phase coherent peaks in the cross section. In general the scattering cross sections have a small isotropic component and four regularly spaced peaks. The peaks that are observed at $\phi_s=0$, 90, 270, and 360° arise from residual Bragg scattering caused by the average periodicity. The residual Bragg scattering peaks remain in the cross section when we change the wavelength of the light to slightly detune the light from the Bragg scattering condition. This is illustrated by the results plotted in Fig. 2(c) for a random system with $a/\lambda=0.9$ that is periodic on average.

B. $C^{(1)}$ and $C^{(10)}$ contributions to the angular speckle correlator

The contributions $C^{(1)}$ and $C^{(10)}$ to the speckle correlator are computed as statistical averages involving the differential scattering cross sections and their products. These contributions dominate $C(\vec{q},\vec{k}|\vec{q}',\vec{k}')$ since they occur in the lowest order scattering processes yielding a contribution to $C(\vec{q},\vec{k}|\vec{q}',\vec{k}')$. A comparison of $C^{(1)}$ and $C^{(10)}$ is made for the two types of model disorder and in some cases for several values of ϵ.

In homogeneous random systems, the $C^{(1)}(\vec{q},\vec{k}|\vec{q}',\vec{k}')$ contribution has been shown to be nonzero only for processes that satisfy $\vec{q}-\vec{k}-\vec{q}'+\vec{k}'=0$, and the $C^{(10)}(\vec{q},\vec{k}|\vec{q}',\vec{k}')$ contribution has been shown to be nonzero only for processes that satisfy the wave-vector condition $\vec{q}-\vec{k}+\vec{q}'-\vec{k}'=0$. We first make some simulation studies that identify $C^{(1)}$ and $C^{(10)}$ as the dominant contributions to the speckle correlator in the homogeneous random system, and verify that $C^{(1)}$ and $C^{(10)}$ occur for wave vectors that satisfy these two conditions. To do this computer simulation runs

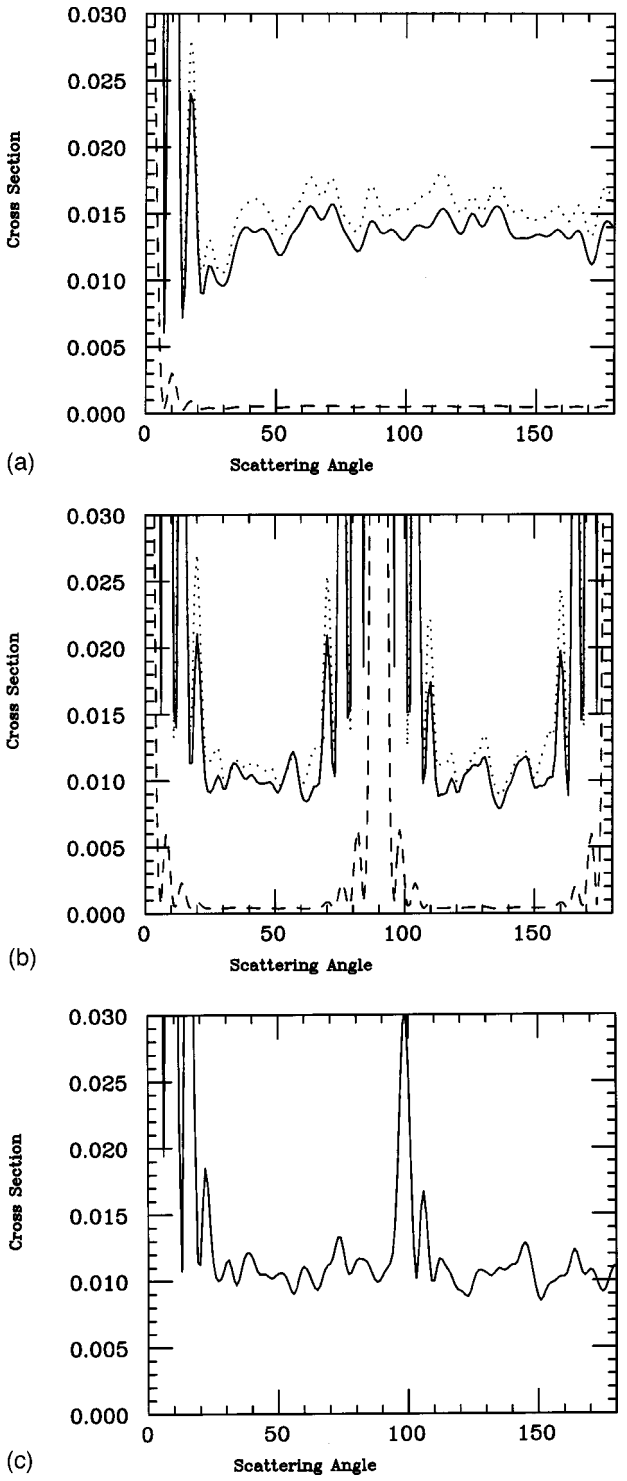

FIG. 2. (a) Differential scattering cross section versus azimuthal scattering angle ϕ_s for a uniformly random system. Results are shown for systems with $R/\lambda=0.064$, $\epsilon=-9$ (solid line), 2 (dashed line), and 9 (dotted). Note that the dotted line results have been multiplied by 0.1 to fit on the scale of the figure. (b) Differential scattering cross section for the periodic on average system with $a/\lambda=1$ and $R/\lambda=0.064$. The notation is the same as in (a). (c) Differential scattering cross section for the periodic on average system for $a/\lambda=0.9$, $R/\lambda=0.064$ for $\epsilon=-9$.

are made in which $\vec{q}$, $\vec{k}$ are fixed and a series of values of $\vec{q}'$ and $\vec{k}'$ are scanned through. During the scan, maxima are observed in the speckle correlator when either or both of the two wave-vector conditions given above are satisfied. These maxima correspond to the $C^{(1)}$ and $C^{(10)}$ contributions to the speckle correlator. Similar scans are made on the periodic on average system. The periodic on average system is found to exhibit additional peaks in $C^{(1)}$ and $C^{(10)}$ for $\vec{q}-\vec{k}-\vec{q}'+\vec{k}'\neq 0$ and for $\vec{q}-\vec{k}+\vec{q}'-\vec{k}'\neq 0$ that are not found in these functions for the homogeneous random system. The origins of these peaks will be discussed in Sec. III C.

In Fig. 3 results are presented of a scan on $\vec{q}'$, $\vec{k}'$ for fixed $\vec{q}$, $\vec{k}$ for $C(\vec{q},\vec{k}|\vec{q}',\vec{k}')$ in the homogeneous disordered system. Plots for a number of different positive and negative values of ϵ are shown. The wave vectors of the incident and scattered light are taken to be in the $x-y$ plane and are of the form

$$\vec{k}=k_0(1,0,0), \tag{20}$$

$$\vec{k}'=k_0(\cos\phi,\sin\phi,0), \tag{21}$$

$$\vec{q}=k_0(0,1,0), \tag{22}$$

$$\vec{q}'=k_0(\sin\phi,-\cos\phi,0). \tag{23}$$

Here the azimuthal angle ϕ runs from 0 to 360°. The plots have maxima at $\phi=90°$, corresponding to wave vectors that satisfy $\vec{q}-\vec{k}+\vec{q}'-\vec{k}'=0$ for a nonzero $C^{(10)}$. A second set of maxima are found at $\phi=270°$ and satisfy $\vec{q}-\vec{k}-\vec{q}'+\vec{k}'=0$ for nonzero $C^{(1)}$. Figure 3 clearly display, the contributions of both $C^{(1)}$ and $C^{(10)}$ to the speckle correlator. It is interesting to note that the results for $|\epsilon|=9$ exhibit peaks in the correlator scans that are similar to the results for $|\epsilon|=2$. The intensities of these correlators, however, are quite different.

In Fig. 4 results are presented as in Fig. 3, but for a random system that is periodic on average. The wave vectors and the angle ϕ are defined as in Eqs. (20)–(23), and the average periodicity is defined such that $a/\lambda=1$. Unlike the homogeneous random system, in the scan over ϕ the periodic on average system displays four peaks instead of two peaks. The two additional peaks at $\phi=180°$ and 360° arise from the average periodicity of the array of spheres, and correspond to scattering sequences in which at least one Bragg reflection is involved. A further discussion of the origin of of these peaks will be given below in subsection C. Well defined peaks are observed in the $|\epsilon|=9$ plots, but a more complicated behavior involving a central peak with side dips is found in the $|\epsilon|=2$ plots. The widths and side peaks observed in Figs. 3 and 4 are for angular scans passing though, not along, the envelopes of $C^{(1)}$ and $C^{(10)}$, and arise from finite-size effects. For an infinite sample the central peaks would become delta functions and the side peaks would disappear. For finite-sized samples, the side peaks arise from diffractive effects due to the finite sample size.

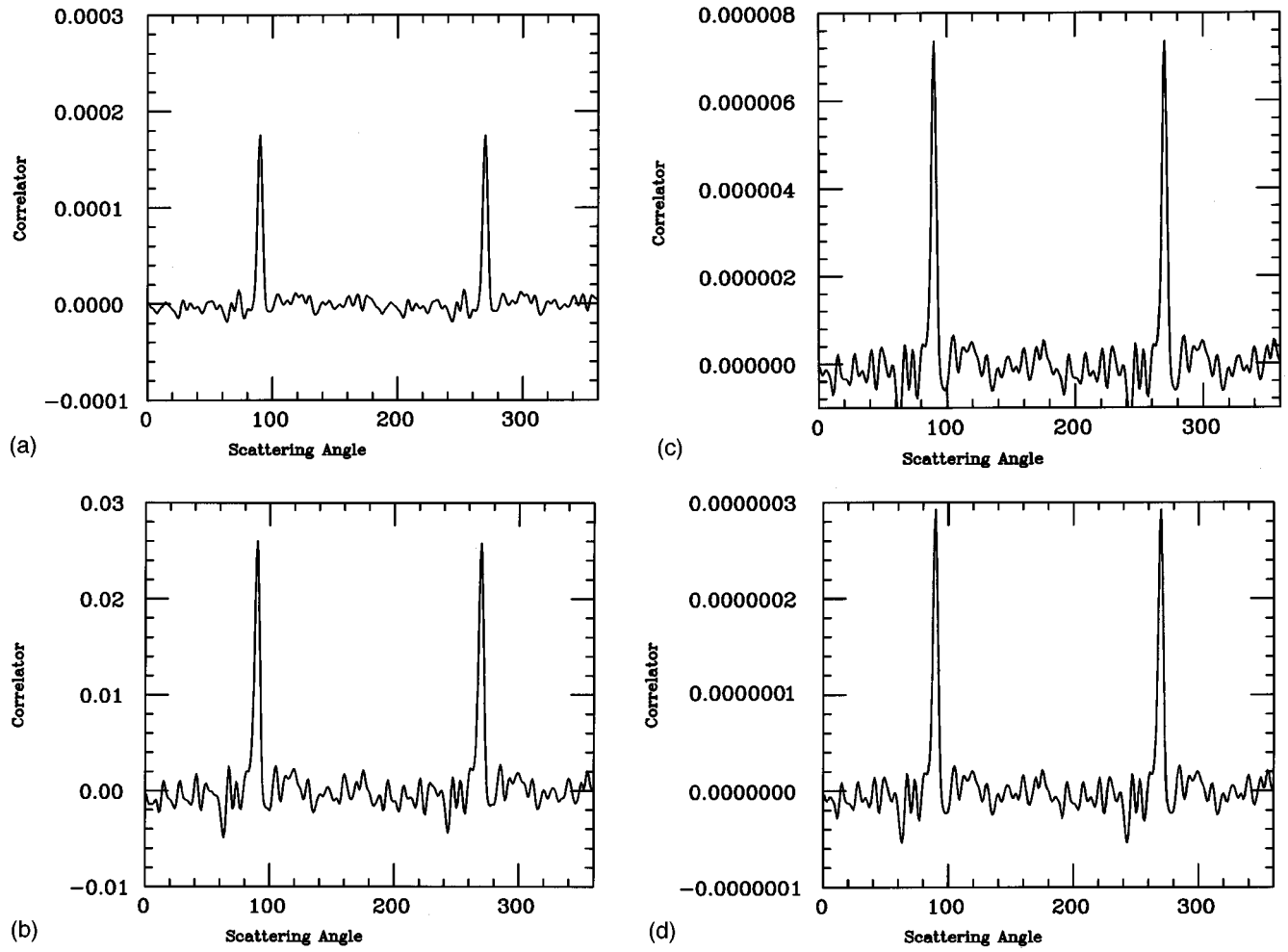

FIG. 3. $C(\vec{q},\vec{k}|\vec{q}',\vec{k}')$ versus the scattering angle ϕ for the uniformly disordered system. Results are shown for $\epsilon=$: (a) -9; (b) 9; (c) -2; and (d) 2.

Figures 3 and 4 exhibit the existence of the $C^{(1)}$ and $C^{(10)}$ functions, which are nonzero when $\vec{q}-\vec{k}-\vec{q}'+\vec{k}'=0$ and $\vec{q}-\vec{k}+\vec{q}'-\vec{k}'=0$, respectively. We now look at the envelopes of these functions. The envelopes are obtained as $\vec{q}$, $\vec{k}$, $\vec{q}'$, $\vec{k}'$ are varied so that either or both of the conditions $\vec{q}-\vec{k}-\vec{q}'+\vec{k}'=0$, $\vec{q}-\vec{k}+\vec{q}'-\vec{k}'=0$ are always satisfied.

Results are first presented for the envelope function of $C^{(1)}$. We account for the $\vec{q}-\vec{k}-\vec{q}'+\vec{k}'=0$ restriction on $C^{(1)}(\vec{q},\vec{k}|\vec{q}',\vec{k}')$ by writing

$$\vec{k}=k_0(\sin\theta,0,\cos\theta), \tag{24}$$

$$\vec{k}'=k_0(\sin\theta,0,-\cos\theta), \tag{25}$$

$$\vec{q}=k_0(\sin\theta\cos\phi,\sin\theta\sin\phi,\cos\theta), \tag{26}$$

$$\vec{q}'=k_0(\sin\theta\cos\phi,\sin\theta\sin\phi,-\cos\theta). \tag{27}$$

In this representation $\vec{q}-\vec{k}$ and $\vec{q}'-\vec{k}'$ are parallel vectors that are sent into one another by reflection through the $x-y$ plane. They lie on chords of the sphere of radius k_0 centered at the origin of coordinates in wave-vector space. This is a natural way to choose vectors satisfying $\vec{q}-\vec{k}-\vec{q}'+\vec{k}'=0$.

In Fig. 5 the speckle correlator of the homogeneous random system is shown as a function of the polar angle θ for fixed azimuthal angles $\phi=0$, 20, and 90°. For the choice of wave vectors in Eqs. (24)–(27), the correlator is symmetric under reflection through the $x-y$ plane so that results are shown only for $0\leqslant\theta\leqslant 90°$. For $\phi=0°$, peaks are observed at $\theta=0°$ and $\theta=90°$. These correspond to light that is scattered along time reversed $[\vec{q}=\vec{k}=-\vec{q}'=-\vec{k}'=k_0(0,0,1)]$ and same sequence scattering $[\vec{q}=\vec{k}=\vec{q}'=\vec{k}'=k_0(1,0,0)]$ paths, respectively. It is expected in Fig. 5 and the other figures presented in this paper that time reversed and same sequence scattering process may lead to enhanced correlations. In the case of same sequence scattering, two waves that undergo exactly the same scattering process in traversing a disordered medium should undergo the same change in phase from the initial to the final scattering. This retention of the phase difference before and after scattering should contribute to a constructive interference in the intensity which would tend to increase the intensity correlator when same

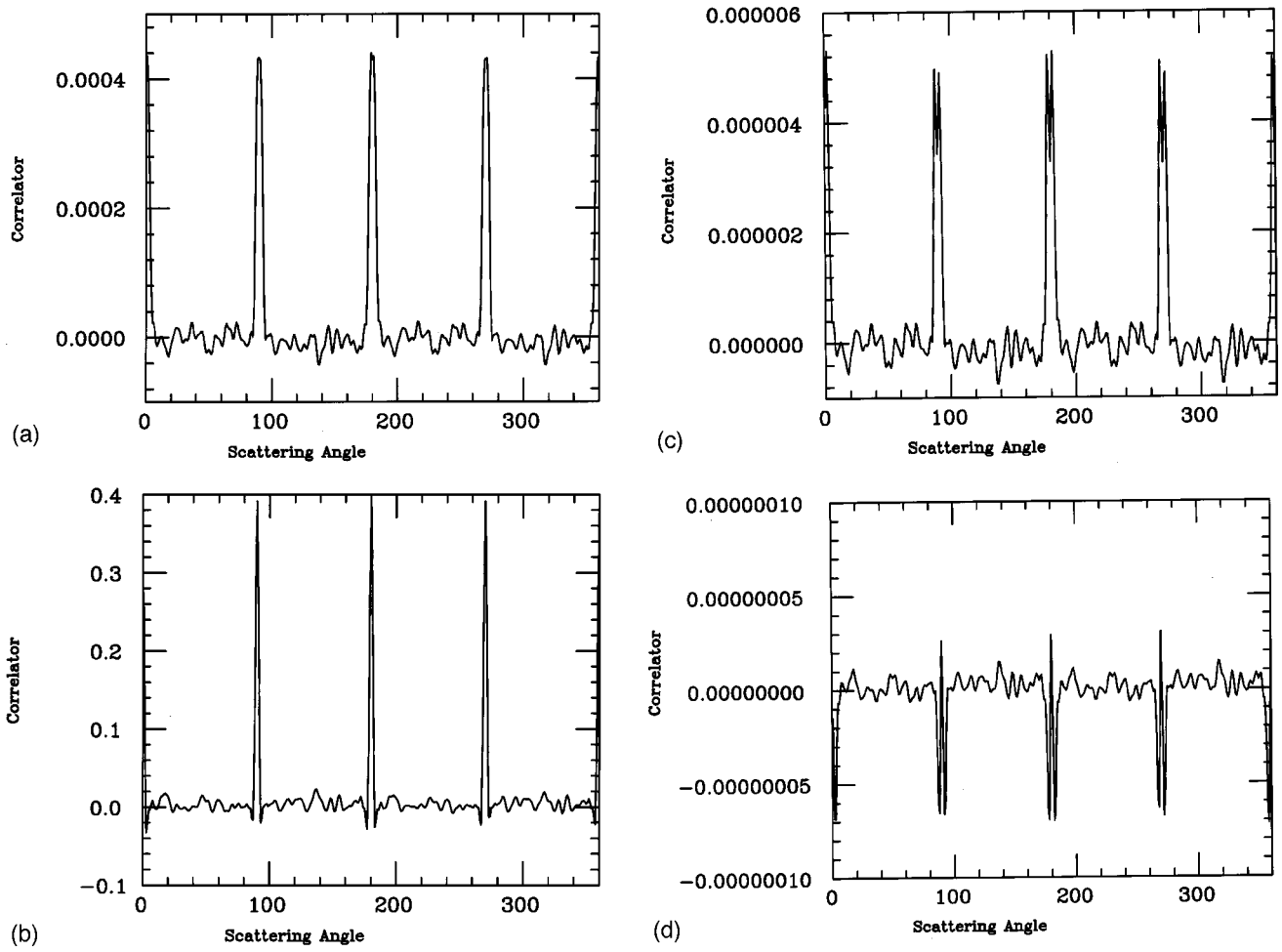

FIG. 4. $C(\vec{q},\vec{k}|\vec{q}',\vec{k}')$ versus the scattering angle ϕ for the periodic on average system. Results are shown for $\epsilon=$: (a) -9; (b) 9; (c) -2; and (d) 2.

sequence scattering process are possible. Same sequence scattering processes can only occur for a restricted range of $\vec{q}$, $\vec{q}'$, $\vec{k}$, and $\vec{k}'$ values. Likewise, for time reversed processes two waves encounter the scatterers of the medium in an exactly reversed sequence, and the retention of the relative phase difference of the two waves is expected to enhance the intensity correlations between the processes scattering the two waves. Once again time reversed processes can only occur for a restricted range of $\vec{q}$, $\vec{q}'$, $\vec{k}$, and $\vec{k}'$. For $\phi=20°$, a small peak is observed at $\theta=0°$ corresponding to the time reversed sequence $[\vec{q}=\vec{k}=-\vec{q}'=-\vec{k}'=k_0(0,0,1)]$, but no peak is found associated with the $\theta=90°$ same sequence scattering processes. For $\phi=90°$ a peak structure is observed near the time reversed $\theta=0$ sequence. Otherwise, the $\phi=90°$ correlator is a smoothly varying function of θ. It is noted in these plots that both $C^{(1)}$ and $C^{(10)}$ are nonzero at general ϕ for $\theta=0°$ and at $\phi=90°$ for $\theta=90°$. At these points the correlator has contributions from both the $C^{(1)}$ and $C^{(10)}$ processes.

To study the $C^{(10)}(\vec{q},\vec{k}|\vec{q}',\vec{k}')$ contribution to the angular speckle correlator, the $\vec{q}-\vec{k}+\vec{q}'-\vec{k}'=0$ restriction on the wave vectors $\vec{q},\vec{k},\vec{q}',\vec{k}'$ is accounted for by writing

$$\vec{k}=k_0(\sin\theta,0,\cos\theta), \tag{28}$$

$$\vec{k}'=k_0(-\sin\theta,0,\cos\theta), \tag{29}$$

$$\vec{q}=k_0(\sin\theta\cos\phi,\sin\theta\sin\phi,\cos\theta), \tag{30}$$

$$\vec{q}'=k_0(-\sin\theta\cos\phi,-\sin\theta\sin\phi,\cos\theta). \tag{31}$$

The vectors $\vec{q}-\vec{k}$ and $\vec{q}'-\vec{k}'$ are now antiparallel vectors in a plane of constant polar angle of the sphere of radius k_0 centered at the origin of coordinates in wave-vector space, and occupy parallel chords of the sphere. This is again a natural representation for wave vectors that satisfy $\vec{q}-\vec{k}+\vec{q}'-\vec{k}'=0$. Here θ is the polar angle of the plane containing $\vec{q}-\vec{k}$ and $\vec{q}'-\vec{k}'$, and ϕ is the azimuthal angle in this plane.

The results for $C^{(10)}(\vec{q},\vec{k}|\vec{q}',\vec{k}')$ are plotted in Fig. 6 versus θ for $\phi=0$, 20, and 90°. These results are, again, invariant under reflection in the $x-y$ plane so that results are shown only for $0\leqslant\theta\leqslant90°$. For the case in which $\phi=0°$ peaks are observed for $\theta=0°$ corresponding to $\vec{q}=\vec{k}=\vec{q}'$

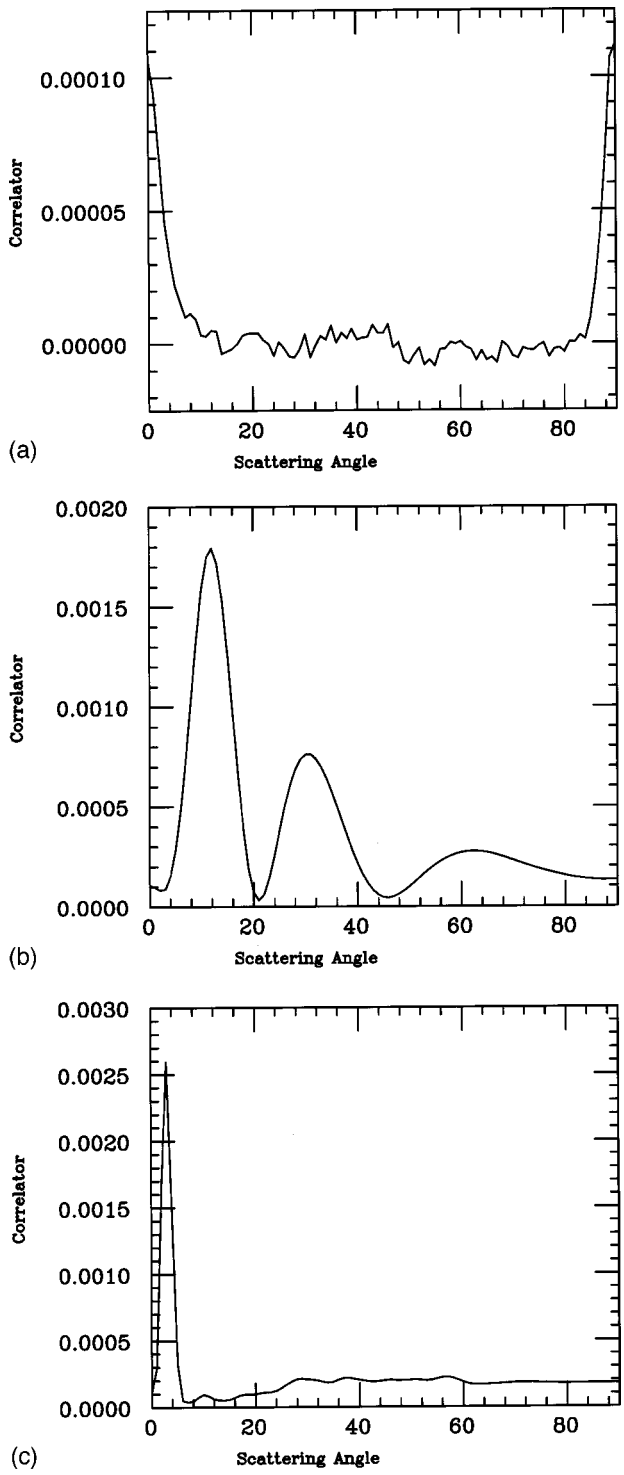

FIG. 5. $C(\vec{q},\vec{k}|\vec{q}',\vec{k}')$ versus θ for the uniformly disordered system. Results are shown for $\phi=$: (a) 0°; (b) 20°; and (c) 90°.

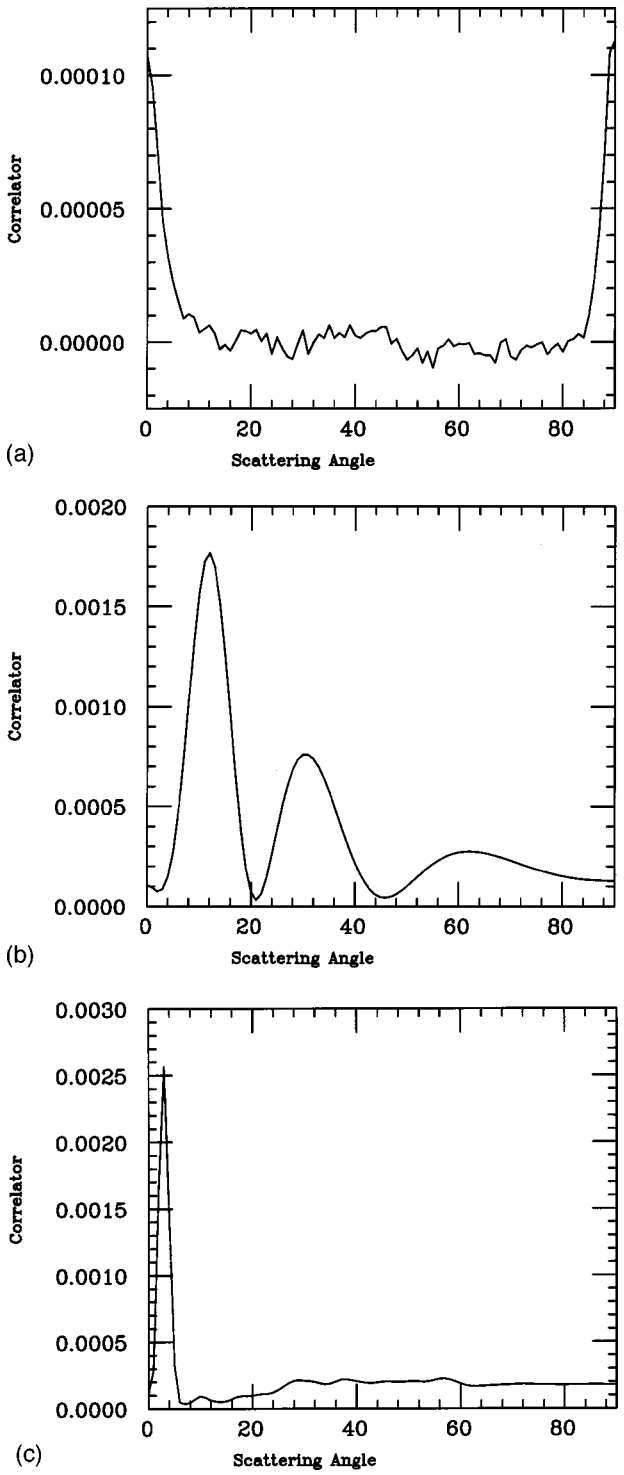

FIG. 6. $C(\vec{q},\vec{k}|\vec{q}',\vec{k}')$ versus θ for the uniformly disordered system. Results are shown for $\phi=$: (a) 0°; (b) 20°; and (c) 90°.

$=\vec{k}'=k_0(0,0,1)$ (same sequence scattering), and for $\theta=90°$ corresponding to $\vec{q}=\vec{k}=-\vec{q}'=-\vec{k}'=k_0(1,0,0)$ (time reversed scattering). At these points, in addition to the phase coherence of the same sequence and time reversed scattering processes, as per our discussion of Fig. 5, both $C^{(1)}$ and $C^{(10)}$ scattering processes make nonzero contributions to $C(\vec{q},\vec{k}|\vec{q}',\vec{k}')$, and the increase in the number of types of correlated scattering processes contributes to an enhancement of $C(\vec{q},\vec{k}|\vec{q}',\vec{k}')$. For general ϕ and $\theta=0°$ both $C^{(1)}$ and $C^{(10)}$ are nonzero and arise from same sequence scattering paths. Peaks are generally observed in Figs. 6 at $\theta=0°$.

In Figs. 7 and 8 we present results for the periodic on average system corresponding to those in Figs. 5 and 6, respectively, for the homogeneous random system. In these

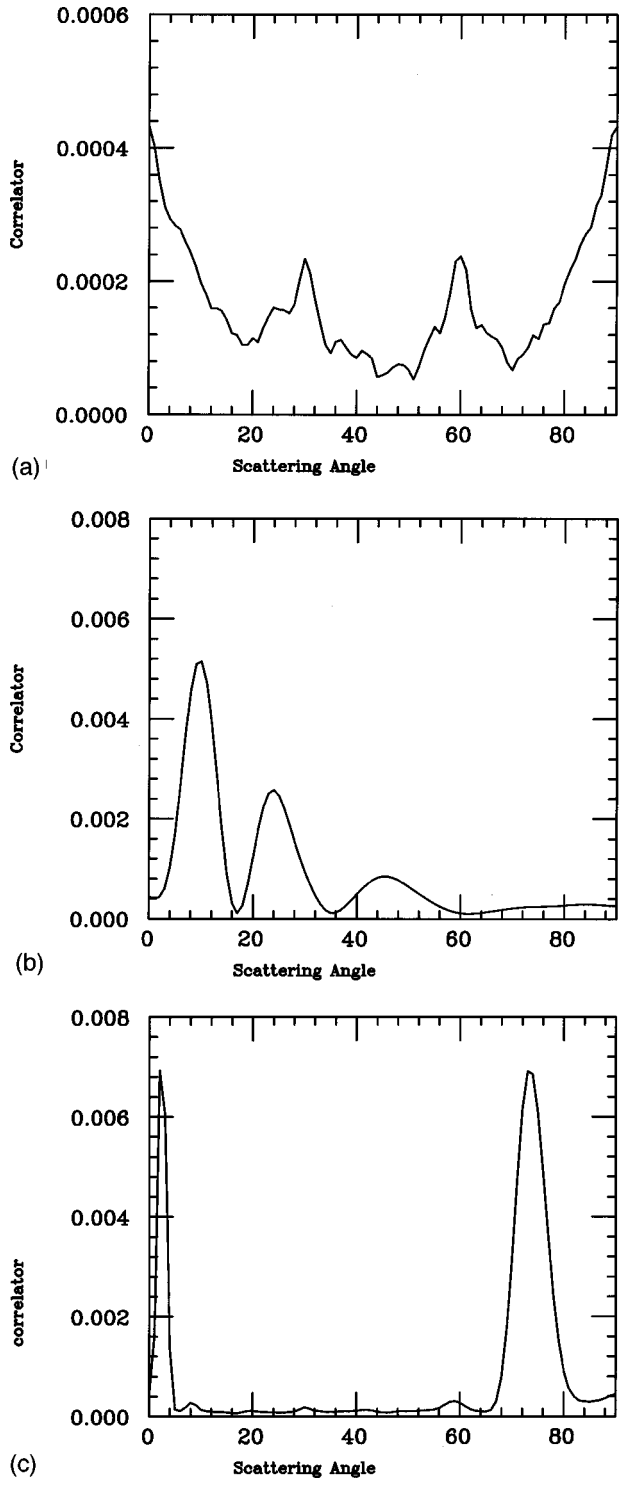

FIG. 7. Results as in Fig. 5 but for the periodic on average system.

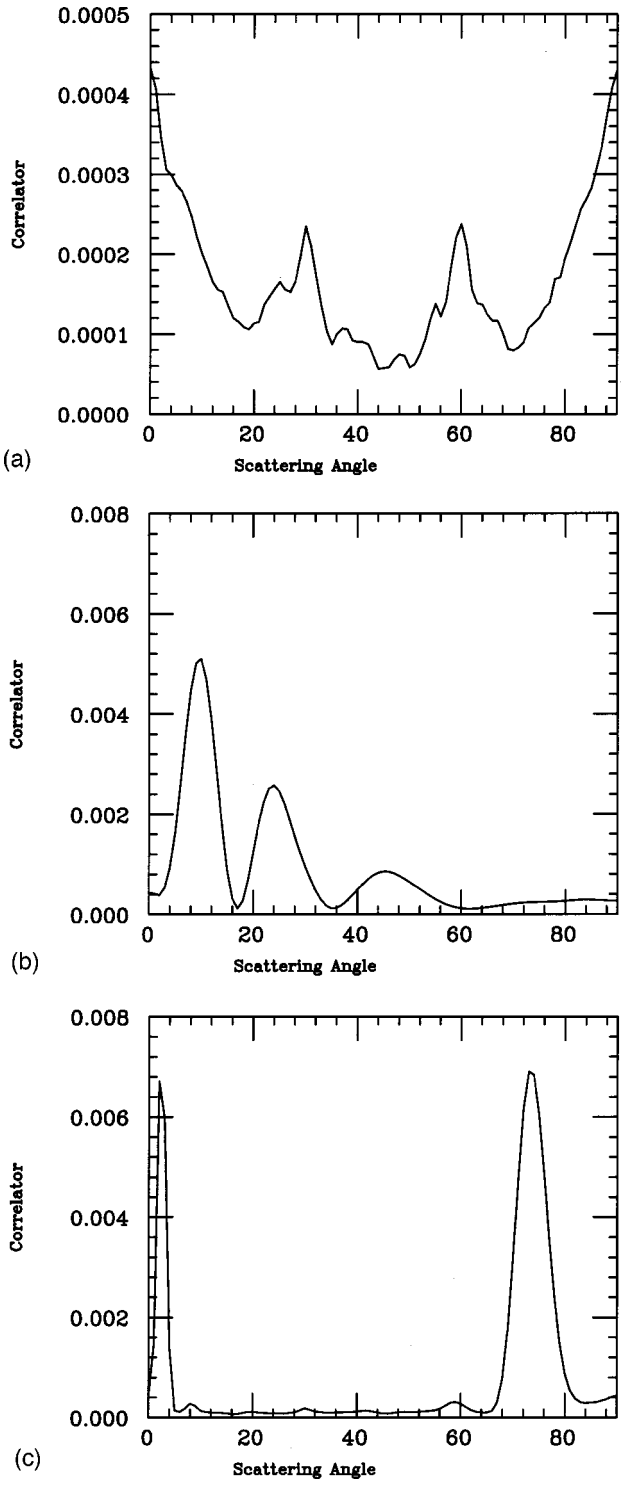

FIG. 8. Results as in Fig. 6 but for the periodic on average system.

plots either or both of the conditions $\vec{q}-\vec{k}-\vec{q}'+\vec{k}'=0$ or $\vec{q}-\vec{k}+\vec{q}'-\vec{k}'=0$ are satisfied. The plots are very similar to the results for the uniform isotropic system. An exception is the $\phi=90°$ results for both $C^{(1)}$ and $C^{(10)}$. For this case peaks are observed for $C^{(1)}$ along a same sequence path and for $C^{(10)}$ along paths of antiparallel incident and scattering beams. Associated with these peaks are two large side peaks arising from residual Bragg scattering effects.

Finally, we note that in plotting the envelope functions in Figs. 5–8 we fixed the azimuthal angle, ϕ, of the vectors $\vec{q}$, $\vec{k}$, $\vec{q}'$, $\vec{k}'$ and scanned over the polar angle θ. As a results of this the differences $\vec{q}-\vec{k}$ and $\vec{q}'-\vec{k}'$ change with changing

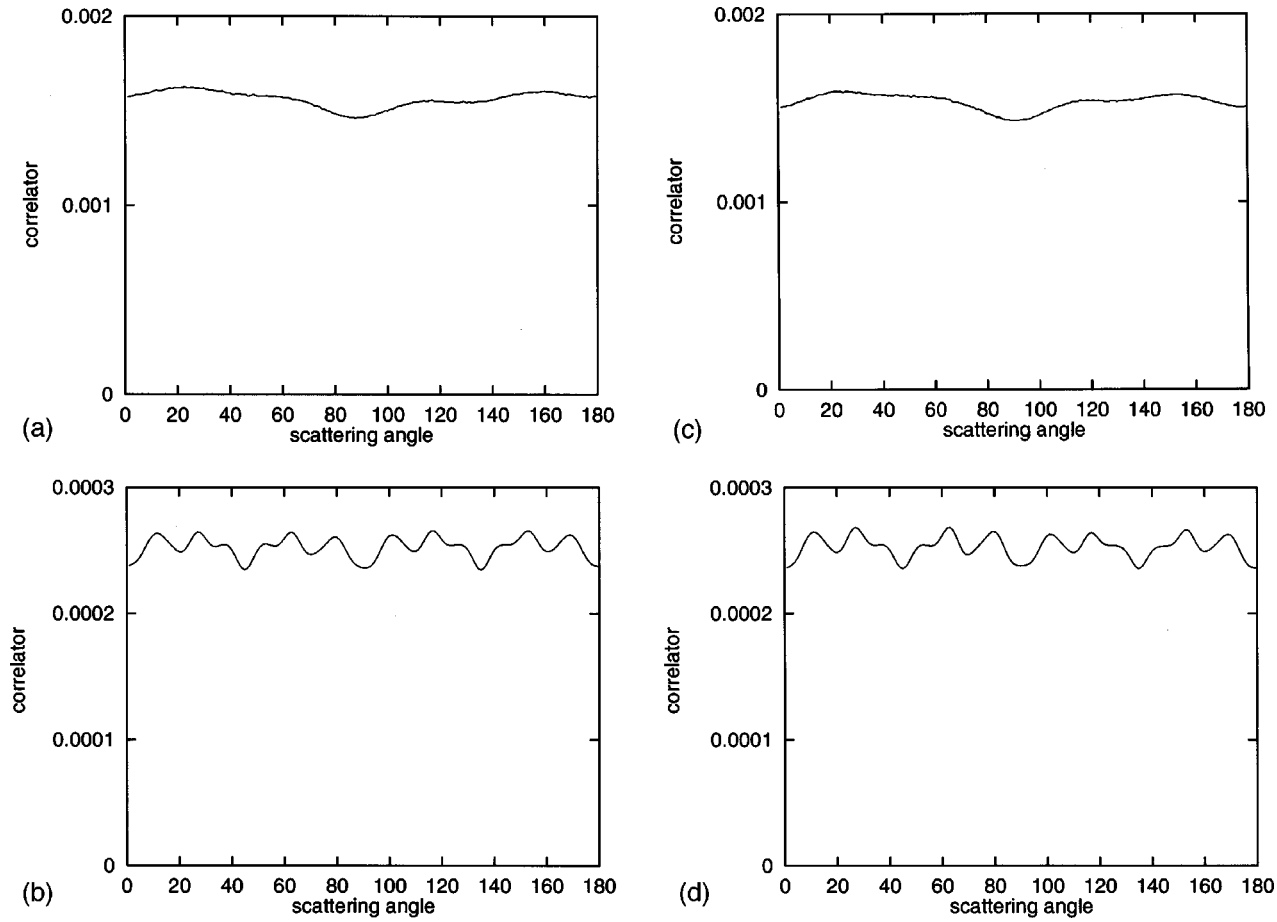

FIG. 9. Plot of the angular speckle correlator for the system of Fig. 4(a). Plots as functions of ϕ are presented for the wave vectors defined in Eqs. (32)–(35) for: (a) $\theta=10°$; (b) $\theta=45°$; and for the wave vectors defined in Eqs. (36)–(39) for: (c) $\theta=10°$; (d) $\theta=45°$.

polar angle. While this samples a wide range of behaviors of the correlators in $\vec{q}$, $\vec{k}$, $\vec{q}'$, $\vec{k}'$, it is interesting to study the correlators for scans in wave-vector space which involve fixed differences of $\vec{q}-\vec{k}$ and $\vec{q}'-\vec{k}'$. If θ is fixed and ϕ is allowed to vary in the vectors defined by

$$\vec{q}=k_0(\sin\theta,0,\cos\theta), \tag{32}$$

$$\vec{k}=k_0(\sin\theta,0,-\cos\theta), \tag{33}$$

$$\vec{q}'=k_0(\sin\theta\cos\phi,\sin\theta\sin\phi,\cos\theta), \tag{34}$$

$$\vec{k}'=k_0(\sin\theta\cos\phi,\sin\theta\sin\phi,-\cos\theta), \tag{35}$$

a plot of the envelope of $C^{(1)}(\vec{q},\vec{k}|\vec{q}',\vec{k}')$ for $\vec{q}-\vec{k}=\vec{q}'-\vec{k}'=k_0(0,0,2\cos\theta)$ is obtained. In Figs. 9(a) and 9(b) we present results for $C^{(1)}$ versus ϕ from the periodic on average system with $\epsilon=-9$ for scattering processes in which $\theta=10$ and 45°. In general, the correlator is seen to be a smooth slowly varying function of ϕ for both polar angles. If we fix θ and vary ϕ for vectors defined by

$$\vec{q}=k_0(\sin\theta,0,\cos\theta), \tag{36}$$

$$\vec{k}=k_0(\sin\theta,0,-\cos\theta), \tag{37}$$

$$\vec{q}'=k_0(\sin\theta\cos\phi,\sin\theta\sin\phi,-\cos\theta), \tag{38}$$

$$\vec{k}'=k_0(\sin\theta\cos\phi,\sin\theta\sin\phi,\cos\theta), \tag{39}$$

a plot of the envelope of $C^{(10)}(\vec{q},\vec{k}|\vec{q}',\vec{k}')$ for $\vec{q}-\vec{k}=-(\vec{q}'-\vec{k}')=k_0(0,0,2\cos\theta)$ is obtained. In Figs. 9(c) and 9(d) we present results for $C^{(10)}$ versus ϕ from the periodic on average system with $\epsilon=-9$ for scattering processes in which $\theta=10$ and 45°. Again, the correlator is found to be relatively independent of ϕ. Similar behaviors are observed in the random system that is not periodic on average.

C. Discussion of additional peaks arising from an average periodicity

An explanation based on analytic techniques can be given for the new peaks observed in the results for the periodic on average system shown in Fig. 4. (Specifically, these are the peaks occurring at $\phi=0$ and 180°.) This is done by applying diagrammatic Green's-function methods to a model system[10] which, though different from the one described in Eqs. (1)–(3), exhibits a periodic on average randomness that is easier to handle analytically and which is qualitatively similar to that of the periodic on average system discussed in Sec. II.

We consider a form for $\epsilon(\vec{r})$ given by

$$\epsilon(\vec{r}) = u(\vec{r}) + \epsilon_0(\vec{r}), \tag{40}$$

where $u(\vec{r})$ is a periodic function and $\epsilon_0(\vec{r})$ is drawn from a set of Gaussian random functions,[10,14–16] $\{\epsilon_0(\vec{r})\}$. The scattering properties of the system are expressed in terms of $\epsilon(\vec{r})$, and the average scattering properties are then determined by averaging over the set of Gaussian random functions, $\{\epsilon_0(\vec{r})\}$. In Eq. (40), the periodic function $u(\vec{r})$ is represented by

$$u(\vec{r}) = \sum_{\vec{G}} u_{\vec{G}} e^{i\vec{G}\cdot\vec{r}}, \tag{41}$$

where the sum is over the set of reciprocal-lattice vectors $\{\vec{G}\}$ of the average periodic lattice, and the Gaussian random function $\epsilon_0(\vec{r})$ satisfies

$$\langle \epsilon_0(\vec{r}) \rangle = 0, \tag{42}$$

$$\langle \epsilon_0(\vec{r}) \epsilon_0(\vec{r'}) \rangle = \sigma^2 g(|\vec{r} - \vec{r'}|). \tag{43}$$

In Eqs. (42) and (43) $\langle\ \rangle$ indicates an average over the set of Gaussian random functions, and the function $g(|\vec{r}-\vec{r'}|)$ is such that $g(0)=1$ and $\lim_{r\to\infty} g(r) \to 0$.

Following a well-known treatment,[10–12,14–16] it can be shown that the electromagnetic scattering cross section of the system in Eqs. (40)–(43) is proportional to a two-particle Green's function, i.e.,

$$\frac{\partial\sigma(\vec{q},\vec{k})}{\partial\Omega} \propto \langle |G_R(\vec{q},\vec{k})|^2 \rangle. \tag{44}$$

Here the Green's function of the random system, $G_R(\vec{q},\vec{k})$, satisfies the Dyson equation

$$G_R(\vec{q},\vec{k}) = (2\pi)^3 \delta(\vec{q}-\vec{k}) G(\vec{k}) + G(\vec{q}) \int \frac{d^3p}{(2\pi)^3} V(\vec{q}|\vec{p}) G_R(\vec{p},\vec{k}), \tag{45}$$

where $G(\vec{k})$ is the Fourier transform of Eq. (8), and the scattering potential for the dielectric system described in Eqs. (40)–(43) is given by

$$V(\vec{p}|\vec{k}) = v(\vec{p}|\vec{k}) \hat{\epsilon}(\vec{p}-\vec{k}). \tag{46}$$

In Eq. (46) $\hat{\epsilon}(\vec{q}) = \int d^3r e^{-i\vec{q}\cdot\vec{r}} \epsilon(\vec{r})$, so that from Eqs. (40) and (41)

$$\hat{\epsilon}(\vec{q}) = \sum_{\vec{G}} u_{\vec{G}} (2\pi)^3 \delta(\vec{q}-\vec{G}) + \hat{\epsilon}_0(\vec{q}), \tag{47}$$

where $\hat{\epsilon}_0(\vec{q}) = \int d^3r e^{-i\vec{q}\cdot\vec{r}} \epsilon_0(\vec{r})$, $u_{\vec{G}} = \int_{plc} d^3r e^{-i\vec{G}\cdot\vec{r}}$ and plc indicates that the integral is over a primitive lattice cell. The coefficient $v(\vec{p}|\vec{k})$ in Eq. (46), whose general form is not important to our discussions, contains details of the interaction of the electromagnetic fields with the system which do not affect the gross geometric features of the speckle correlator.

In terms of the Green's function $G_R(\vec{q}|\vec{k})$, it has been shown[1,10–12] that the angular speckle correlator $C^{(1)}(\vec{q},\vec{k}|\vec{q}',\vec{k}')$ satisfies

$$C^{(1)}(\vec{q},\vec{k}|\vec{q}',\vec{k}') \propto \langle G_R^*(\vec{q},\vec{k}) G_R(\vec{q}',\vec{k}') \rangle \times \langle G_R^*(\vec{q}',\vec{k}') G_R(\vec{q},\vec{k}) \rangle - |\langle G_R(\vec{q},\vec{k}) \rangle|^2 |\langle G_R(\vec{q}',\vec{k}') \rangle|^2, \tag{48}$$

and that the angular speckle correlator $C^{(10)}(\vec{q},\vec{k}|\vec{q}',\vec{k}')$ satisfies[10–12]

$$C^{(10)}(\vec{q},\vec{k}|\vec{q}',\vec{k}') \propto \langle G_R^*(\vec{q},\vec{k}) G_R^*(\vec{q}',\vec{k}') \rangle \times \langle G_R(\vec{q}',\vec{k}') G_R(\vec{q},\vec{k}) \rangle - |\langle G_R(\vec{q},\vec{k}) \rangle|^2 |\langle G_R(\vec{q}',\vec{k}') \rangle|^2. \tag{49}$$

An understanding of the gross geometric properties of $C^{(1)}(\vec{q},\vec{k}|\vec{q}',\vec{k}')$ and $C^{(10)}(\vec{q},\vec{k}|\vec{q}',\vec{k}')$ can be obtained by using Eqs. (45)–(47) to expand Eqs. (48) and (49) through terms of order $u_{\vec{G}}\sigma^2$. We now turn to a discussion of these terms.

The two-particle Green's functions in Eqs. (48) and (49) can be written as

$$\langle G_R(\vec{q},\vec{k}) G_R(\vec{q}',\vec{k}') \rangle = (2\pi)^3 \delta(\vec{q}-\vec{k}) G(\vec{k}) (2\pi)^3 \times \delta(\vec{q}'-\vec{k}') G(\vec{q}') + G(\vec{q}) G(\vec{q}') \times \Gamma^0(\vec{q},\vec{k}|\vec{q}',\vec{k}') G(\vec{k}) G(\vec{k}'), \tag{50}$$

and

$$\langle G_R^*(\vec{q},\vec{k}) G_R(\vec{q}',\vec{k}') \rangle = (2\pi)^3 \delta(\vec{q}-\vec{k}) G^*(\vec{k}) (2\pi)^3 \times \delta(\vec{q}'-\vec{k}') G(\vec{q}') + G^*(\vec{q}) G(\vec{q}') \times \Gamma^1(\vec{q},\vec{k}|\vec{q}',\vec{k}') G^*(\vec{k}) G(\vec{k}'), \tag{51}$$

where $\Gamma^0(\vec{q},\vec{k}|\vec{q}',\vec{k}')$ and $\Gamma^1(\vec{q},\vec{k}|\vec{q}',\vec{k}')$ are the respective reducible vertex functions arising from the scattering interaction described by $\langle V(\vec{q}|\vec{k}) V(\vec{q}'|\vec{k}') \rangle$ and $\langle V^*(\vec{q}|\vec{k}) V(\vec{q}'|\vec{k}') \rangle$. Computing the reducible vertex function in Eq. (50) to terms of order $u_{\vec{G}}\sigma^2$, we find the general form

$$\Gamma_0^0(\vec{q},\vec{k}|\vec{q}',\vec{k}') = A(\vec{q},\vec{k}|\vec{q}',\vec{k}') \delta(\vec{q}-\vec{k}+\vec{q}'-\vec{k}') + B(\vec{q},\vec{k}|\vec{q}',\vec{k}') \sum_{\vec{G}} \delta(\vec{q}-\vec{k}+\vec{q}'-\vec{k}'+\vec{G}), \tag{52}$$

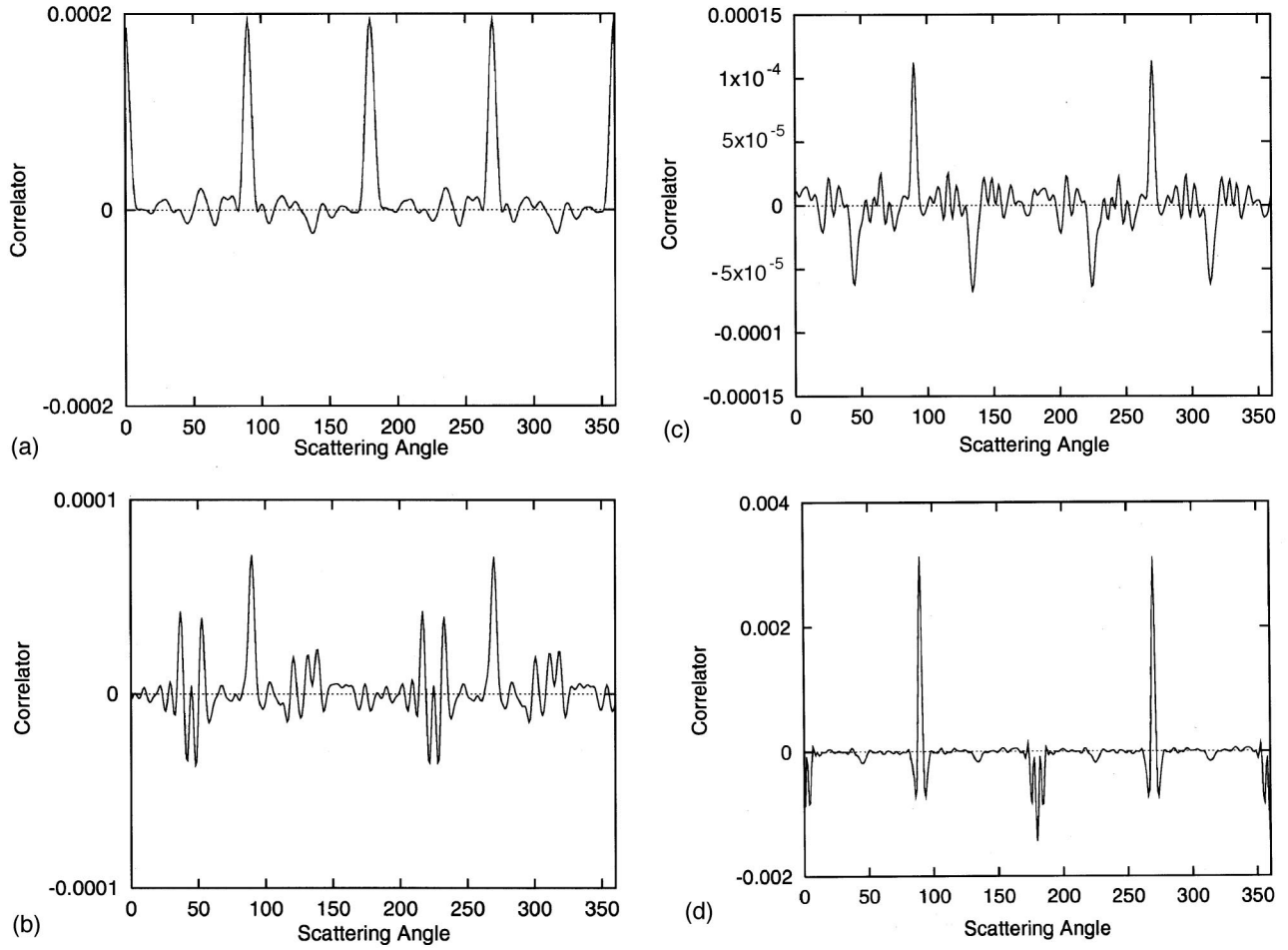

FIG. 10. Results for the angular speckle correlator for the system of Fig. 4(a). Plots are presented for the wave vectors defined in Eqs. (56)–(59) showing the total correlator function as a function of the scattering angle ϕ. Results are shown for: (a) $\theta=30°$; (b) $\theta=45°$; (c) $\theta=50°$; and (d) $\theta=70°$.

where $A(\vec{q},\vec{k}|\vec{q}',\vec{k}')$ and $B(\vec{q},\vec{k}|\vec{q}',\vec{k}')$ are smoothly varying functions of $\vec{q}$, $\vec{k}$, $\vec{q}'$, and $\vec{k}'$. Computing the reducible vertex function in Eq. (51) to terms of order $u_{\vec{G}}\sigma^2$, we find the general form

$$\Gamma_0^1(\vec{q},\vec{k}|\vec{q}',\vec{k}')=D(\vec{q},\vec{k}|\vec{q}',\vec{k}')\,\delta(\vec{q}-\vec{k}-\vec{q}'+\vec{k}') + E(\vec{q},\vec{k}|\vec{q}',\vec{k}')\sum_{\vec{G}}\ \delta(\vec{q}-\vec{k}-\vec{q}'+\vec{k}'+\vec{G}), \tag{53}$$

where $D(\vec{q},\vec{k}|\vec{q}',\vec{k}')$ and $E(\vec{q},\vec{k}|\vec{q}',\vec{k}')$ are smoothly varying functions of $\vec{q}$, $\vec{k}$, $\vec{q}'$, and $\vec{k}'$.

From Eqs. (48)–(53) we see that

$$C^{(1)}(\vec{q},\vec{k}|\vec{q}',\vec{k}')\propto\sum_{\vec{G}}\ \delta(\vec{q}-\vec{k}-\vec{q}'+\vec{k}'+\vec{G}) \tag{54}$$

and

$$C^{(10)}(\vec{q},\vec{k}|\vec{q}',\vec{k}')\propto\sum_{\vec{G}}\ \delta(\vec{q}-\vec{k}+\vec{q}'-\vec{k}'+\vec{G}). \tag{55}$$

The effect on the speckle correlator of the average periodicity in the random system is found in the additional delta-function terms in Eqs. (54) and (55) over the single ($\vec{G}=0$) delta-function terms found in the system that is not periodic on average. In the absence of average periodicity (the $|\vec{G}|\to\infty$ limit), only the $\vec{G}=0$ terms contribute in Eqs. (54) and (55).

To investigate, in the context of our computer simulations discussed in Sec. II, the $\vec{G}\neq 0$ terms in Eqs. (54) and (55), it is useful to take the forms

$$\vec{k}=k_0(\sin\theta,0,\cos\theta), \tag{56}$$

$$\vec{k}'=k_0(\cos\phi\sin\theta,\sin\phi\sin\theta,\cos\theta), \tag{57}$$

$$\vec{q}=k_0(0,\sin\theta,\cos\theta), \tag{58}$$

$$\vec{q}'=k_0(\sin\phi\sin\theta,-\cos\phi\sin\theta,\cos\theta). \tag{59}$$

In the limit that $\theta=90°$ the wave vectors $\vec{k}$, $\vec{k}'$, $\vec{q}$, $\vec{q}'$ in Eqs. (56)–(59) reduce to those given in Eqs. (20)–(23) and reproduce the results in Fig. 4 for the periodic on average system.

For $\theta \neq 90°$ all four vectors have the same z component, and for $\theta = 0°$ all four vectors are parallel to the z axis. Using the wave vectors in Eqs. (56)–(59) we find for general θ and ϕ

$$\vec{q}-\vec{k}-\vec{q}'+\vec{k}' = k_0 \sin\theta(-1-\sin\phi+\cos\phi, 1+\cos\phi + \sin\phi, 0), \tag{60}$$

and

$$\vec{q}-\vec{k}+\vec{q}'-\vec{k}' = k_0 \sin\theta(-1+\sin\phi-\cos\phi, 1-\cos\phi - \sin\phi, 0), \tag{61}$$

which give simple expressions in ϕ and θ for these two important linear combinations of the incident and scattering wave vectors of the angular speckle correlator.

From Eqs. (54) and (55), it is seen that when the right-hand side of either Eq. (60) or (61) becomes equal to a reciprocal-lattice vector, then either $C^{(1)}$ or $C^{(10)}$, respectively, are nonzero. Otherwise, these contributions to the general angular speckle correlator are zero. We shall now use these results to explain the peaks observed in Fig. 4 for the periodic on average system. Following this, we shall present additional results for the periodic on average system considered in Fig. 4 that illustrate the general $\vec{G} \neq 0$ results in Eqs. (54) and (55) for these types of systems.

In Fig. 4 simulation results have been presented for the $\theta = 90°$ case of the wave-vector geometry described by Eqs. (56)–(61). Peaks are observed for $\phi = 0$, 90, 180, and 270°. Upon evaluating Eqs. (60) and (61) for the values of θ and ϕ at which peaks are found in the angular speckle correlator, we find that the four peaks correspond to cases in which the right-hand sides of Eqs. (60) and (61) become equal to reciprocal-lattice vectors. In particular, the peaks observed at $\phi = 0$ and 180° arise from cases in which the right-hand sides of Eqs. (60) and (61) are nonzero reciprocal-lattice vectors, and the peaks at $\phi = 90$ and 270° arise in part from cases in which the right-hand sides of Eqs. (60) and (61) are the zero reciprocal-lattice vector.

In Fig. 10 we extend this analysis to cases in which $\theta \neq 90°$. Scans are presented in ϕ for the angular speckle correlator of the $\epsilon = -9$ periodic on average system treated in Fig. 4(a). Plots are presented of the total correlator $C(\vec{q},\vec{k}|\vec{q}',\vec{k}')$ versus ϕ for $\theta = 30$, 45, 50, 70°, and a variety of peaks and dips are observed as a function of ϕ in these plots. Evaluating Eqs. (60) and (61) we find that the four peaks in the $\theta = 30°$ plot occur when the right-hand sides of Eqs. (60) or (61) equal vectors of the reciprocal lattice. The peaks at $\phi = 0°$ and 180° arise from nonzero reciprocal-lattice vectors, and are consequently absent in the system that is not periodic on average. The peaks at $\phi = 90$ and 270° arise in part from $\vec{G} = 0$ and will be found in the results for the homogeneous random system. From Eqs. (60) and (61) we find that the peaks in the $\theta = 45°$ plot located about $\phi = 0$, 90, 180, 270° occur for cases where Eqs. (60) or (61) become equal to reciprocal-lattice vectors, and the peaks located about $\phi = 45$, 135, 225°, occur for cases in which the right-hand sides of Eqs. (60) or (61) are close to, but not quite equal to, reciprocal-lattice vectors. From Eqs. (60) and (61) we find that the peaks or dips in the $\theta = 50$ and 70° plots for the peaks or dips at $\phi = 45$, 90, 135, 225, 270, 315° occur for cases in which the right-hand side of Eqs. (60) or (61) are close to reciprocal-lattice vectors.

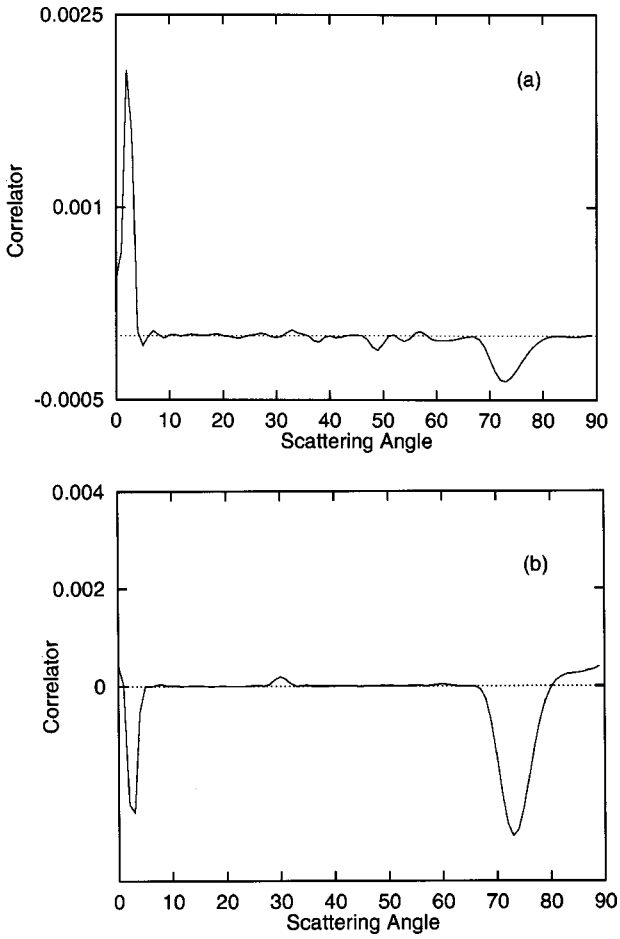

FIG. 11. Results for the angular speckle correlator for the same system as considered in Fig. 10, now plotted as a function of the scattering angle θ for fixed values of: (a) $\phi = 45°$; and (b) $\phi = 180°$.

The delta functions in Eqs. (54) and (55) represent results for an ideal random system that is of infinite extent. For random systems of finite extent we expect that the delta function in Eqs. (54) and (55), $\delta(\vec{q}-\vec{k}-\vec{q}'+\vec{k}'+\vec{G})$ and $\delta(\vec{q}-\vec{k}+\vec{q}'-\vec{k}'+\vec{G})$, are replaced by peaked functions $f(\vec{q}-\vec{k}-\vec{q}'+\vec{k}'+\vec{G})$ and $f(\vec{q}-\vec{k}+\vec{q}'-\vec{k}'+\vec{G})$ with maxima at the zero of their arguments and widths of order $1/l$ where l is a typical linear size dimension (i.e., the radius of the smallest covering sphere) of the finite system. Consequently, the peaks observed near reciprocal-lattice vectors in the plots for $\theta = 45$, 50, 70° should in some cases become less pronounced as the size of the system increases.

To complement the runs made in Figs. 4 and 10, where plots of ϕ for fixed θ are given, it is interesting to fix ϕ at 45 or 180° and plot the angular speckle correlator for θ running from 0 to 90°. These plots are then analogous to the plots made in Figs. 5–8 for the $\vec{G} = 0$ envelopes. In Fig. 11 results

are presented for the $\epsilon=-9$ periodic on average system studied in Fig. 4(a) for $\phi=45$ and 180° for the speckle correlator as a function of θ. In these plots, anomalous behavior is found near sets of angles for which the right-hand sides of Eqs. (60) and (61) are approximately equal to vectors of the reciprocal lattice. It is interesting to note that in both plots negative dips in the correlator are found near $\theta=70°$.

IV. CONCLUSIONS

We have computed the scattering cross section and the speckle correlator for the far-field scattering of light by a finite, random, array of dielectric spheres. Two different types of randomness are considered. In one, the spheres randomly occupy space uniformly subject to the condition that different spheres do not overlap. In a second, the spheres randomly occupy space with a distribution that is periodic on average. The results presented confirm the existence of both the $C^{(1)}$ contribution to the speckle correlator (which has been known to exist from a number of publications[1–12]) and the $C^{(10)}$ contribution to the speckle correlator (which has recently been predicted in three-dimensional scattering[10] but only as yet measured in the light scattered from rough metal surfaces[19]). The simulation has been used to determine the envelope function of these correlators. The envelope functions of $C^{(1)}$ and $C^{(10)}$ are seen to be similar to one another when plotted in the angular variables we have used. Interesting additional features are observed both in $C^{(1)}$ and $C^{(10)}$ when an average periodicity is introduced into the randomness of the system. For the periodic on average systems additional regions of nonzero $C^{(1)}$ and $C^{(10)}$, other that those defined by the conditions $\vec{q}-\vec{k}-\vec{q}'+\vec{k}'=0$ and $\vec{q}-\vec{k}+\vec{q}'-\vec{k}'=0$, are observed, that are caused by scatterings involving one or more Bragg reflections.

In conclusion, we note that recently a contribution to the speckle correlator from volume scattering has been introduced, called the $C^{(0)}$ correlation function.[17,18] The systems studied in Refs. 17 and 18 differ from the systems studied in the present paper in that the speckle in Refs. 17 and 18 arises from a point or extended source of electromagnetic radiation in the medium, respectively, whereas in this paper the scattered electromagnetic waves arise from incident plane waves. It appears, however, that the diagrams contributing to $C^{(0)}$ are part of a set of diagrams entering into the definition of the $C^{(1.5)}$ contribution to the speckle correlator defined for both surface and volume scattering.[10–12] This is clear from the characterization of the $C^{(1.5)}$ diagrams for volume scattering given in the second paragraph of Sec. III B of Ref. 10. This is to say that $C^{(0)}$ is composed from two two-particle Green's functions that are connected by a line of scattering interaction, and this is part of the class of contributions to $C^{(1.5)}$. The reader is also referred to our earlier paper on surface scattering[12] where the $C^{(1.5)}$ contributions are discussed in Sec. 2.2. We note in this regard that Fig. 2 of Ref. 12 does not explicitly list the $C^{(0)}$ diagrams because Fig. 2 of Ref. 12 was a list, taken from the many diagrams contributing to $C^{(1.5)}$, of contributions to $C^{(1.5)}$ that have peaks. These peaks were the focus of the work in Ref. 12 and the $C^{(0)}$ diagrams, though part of of the $C^{(1.5)}$ contributions, do not display peaks. The $C^{(1.5)}$ correlator is not a topic of the results presented in this paper, and we will not pursue this topic further here.

ACKNOWLEDGMENTS

The research of A.A.M. was supported in part by Army Research Office Grant DAAD 19-99-1-0321.

[1] B. Shapiro, Phys. Rev. Lett. **57**, 2168 (1986).
[2] S. Feng, C. Kane, P.A. Lee, and A.D. Stone, Phys. Rev. Lett. **61**, 834 (1988).
[3] I. Freund, M. Rosenbluh, and S. Feng, Phys. Rev. Lett. **61**, 2328 (1988).
[4] R. Berkovits, M. Kaveh, and S. Feng, Phys. Rev. B **40**, 737 (1993).
[5] R. Berkovits and M. Kaveh, Phys. Rev. B **41**, 2635 (1990).
[6] L. Wang and S. Feng, Phys. Rev. B **40**, 8284 (1989).
[7] R. Berkovits, Phys. Rev. B **42**, 10 750 (1990).
[8] N. Garcia and A.Z. Genack, Phys. Rev. Lett. **63**, 1678 (1989).
[9] M.P. van Albada, J.F. De Boer, and A. Lagendijk, Phys. Rev. Lett. **64**, 2787 (1990).
[10] V. Malyshkin, A.R. McGurn, and A.A. Maradudin, Phys. Rev. B **59**, 6167 (1999).
[11] V. Malyshkin, A.R. McGurn, T.A. Leskova, A.A. Maradudin, and M. Nieto-Vesperinas, Opt. Lett. **22**, 946 (1997).
[12] V. Malyshkin, A.R. McGurn, T.A. Leskova, A.A. Maradudin, and M. Nieto-Vesperinas, Waves Random Media **7**, 479 (1997).
[13] M. Nieto-Vesperinas, *Scattering and Diffraction in Physical Optics* (John Wiley and Sons, Inc., New York, 1991).
[14] G. Brown, V. Celli, M. Haller, and A. Marvin, Surf. Sci. **136**, 136 (1984).
[15] A.R. McGurn, A.A. Maradudin, and V. Celli, Phys. Rev. B **31**, 4866 (1985).
[16] A.R. McGurn and A.A. Maradudin, J. Opt. Soc. Am. B **4**, 910 (1987).
[17] B. Shapiro, Phys. Rev. Lett. **83**, 4733 (1999).
[18] S.E. Skipetrov and R. Maynard, Phys. Rev. B **62**, 886 (2000).
[19] C.S. West and K.A. O'Donnell, Phys. Rev. B **59**, 2393 (1999).